

# Determination of Filter Criteria for Micro-Meteor Observations by the Arecibo 430 MHz Incoherent Scatter Radar

James Cline, Patryk Giza, Daniel Kellett, Michelle Kojs  
Miami University

## Abstract

The paper discusses filtering of processed incoherent scatter radar (ISR) data, which was collected from the Arecibo 430 MHz ISR in order to detect meteors entering the ionosphere. From the ISR data received, we found that extracting only data from altitudes of 80 km to 130 km and velocities between 2 km/s and 90 km/s provides a good model of meteor phenomena. Variances in the observed phase shift in excess of 1 radian and abnormally large signal-to-noise ratio (SNR) were found to be indicative of interference. These filtering criteria produce accurate data on micro-meteor trends and could be used to determine a mathematical model for micro-meteors

## Introduction

Everyday millions of meteors travel through the earth's atmosphere. These meteors are usually small enough that they burn up in the atmosphere before coming so near to be of concern to us on the ground. However, they are the reason for trace metals in the upper atmosphere<sup>[4]</sup>, and the ionized trails they leave can be used to measure atmospheric winds<sup>[5]</sup>. Knowing the general patterns of micro-meteors is useful for better understanding these phenomena.

Beyond this, there has been much interest in the observation of the ionosphere for a variety of reasons including communication<sup>[6]</sup>, understanding space weather<sup>[6]</sup> as well as over the horizon radar<sup>[7]</sup>. However, these applications are typically made through use of radar, and meteors prove to be a source of major interference with these observations and make further interpretation impossible<sup>[3]</sup>. Thus it is desirable to determine ways to filter out and avoid this interference.

For both of these problems, one of the first steps necessary for providing a solution is to determine reliable criteria for identifying meteors. After criteria for valid meteor observations have been determined, data can be examined and compared with previously gathered data to ensure the accuracy of these criteria. Finally, these criteria can be applied to determine possible ways of avoiding meteors and filtering out meteor interference as appropriate.

Arecibo Observatory (AO) utilizes radar to observe phenomenon in the ionosphere. These radio pulses are transmitted at a given frequency to the area above the telescope, known as the beamwidth. The pulses typically scatter in all directions off of any object in the dish's beamwidth and in the ionosphere the pulses are most commonly scattered by ionized electrons<sup>[1]</sup>. Most meteors observed in the 80 to 120 km range are quite small (1  $\mu\text{g}$ ) so not many radio pulses can be reflected off of the meteor<sup>[2]</sup>. Instead, these meteors create ion trails as they ablate and burn up while traveling through the atmosphere<sup>[3]</sup>. These trails can be classified as either "head" trails (those preceding the meteor) or "tail" trails (the ionized air left behind the meteor). These two types of trails can be detected by radar and analyzed to obtain information about the meteors and the background atmosphere.

Some of the basic information useful to obtain about these received echoes are the heights and velocities of the meteors. The height is determined simply by measuring how long it takes for the radar pulse to be collected by the receiver after having been sent out. The velocity is slightly more complex, relying on Doppler shifts of the transmitted pulses. This also has the limitation of only being able to be measured from a single pulse if the phase of the transmitted pulse is well known. However, as is often the case, such precision in transmitting at exactly the same phase or being able to measure the phase of each transmitted pulse is not possible. Therefore, the shift in phase of multiple consecutive pulses are averaged to determine the Doppler shift and the average velocity of the target<sup>[14]</sup>.

The method of obtaining the data and the aspects of the data used to determine suitable filters is described in section 2. Section 3 presents the results as a collection of graphs, elaborates on how the filter criteria were determined, and discusses how well the filtered data agrees with previous statistical observations of micro-meteors. Our conclusions from these findings can be found in section 4. Finally, section 5 includes acknowledgments and references used.

## **Project Description and Procedure**

Arecibo Observatory was utilized in this experiment, where measurements began January 2nd, 2015 at 1530 AST and concluded on January 4th, 2015 at 1600 AST. The data collection began at 1530, but the first meteors were observed at 1800.

The operating frequency of the Arecibo Observatory is 430 MHz, meaning that the frequency band for AO is Ultra-High frequency (UHF). Both the transmitter and the receiver operate at 430 MHz. A pulse is sent out from the transmitter and received by the receiver. The received radar pulse is unusable until it has gone through signal processing. Figure 1 shows a block diagram of simple pulsed monostatic radar, using the operating frequency at AO.

First, a pulse waveform is created by the waveform generators. Then this pulse waveform is sent to the transmitter, which modulates it to the desired radio frequency, at Arecibo this is 430 MHz, and "amplifies the signal to a useable power level"<sup>[14]</sup>. This modulated pulse waveform is sent to the duplexer, which is sent to the antenna to be transmitted. The modulated

pulse waveform is then transmitted by the transmitter. The duplexer then receives any returning echoes and sends them to the radar receiver.

The first step to the radar receiver is a low-noise radar frequency (RF) amplifier. The received signal is then modulated “to successively lower intermediate frequencies (IFs) and “then to baseband, 0Hz<sup>[14]</sup>. This signal, that is at baseband, is then sent to the data processor, which performs “functions such as pulse compression, matched filtering, Doppler filtering, integration, and motion compensation”<sup>[14]</sup>. The output from the data processor is then sent to the display<sup>[14]</sup>. This is the full process that Arecibo Observatory radar completes in order to read the received signal.

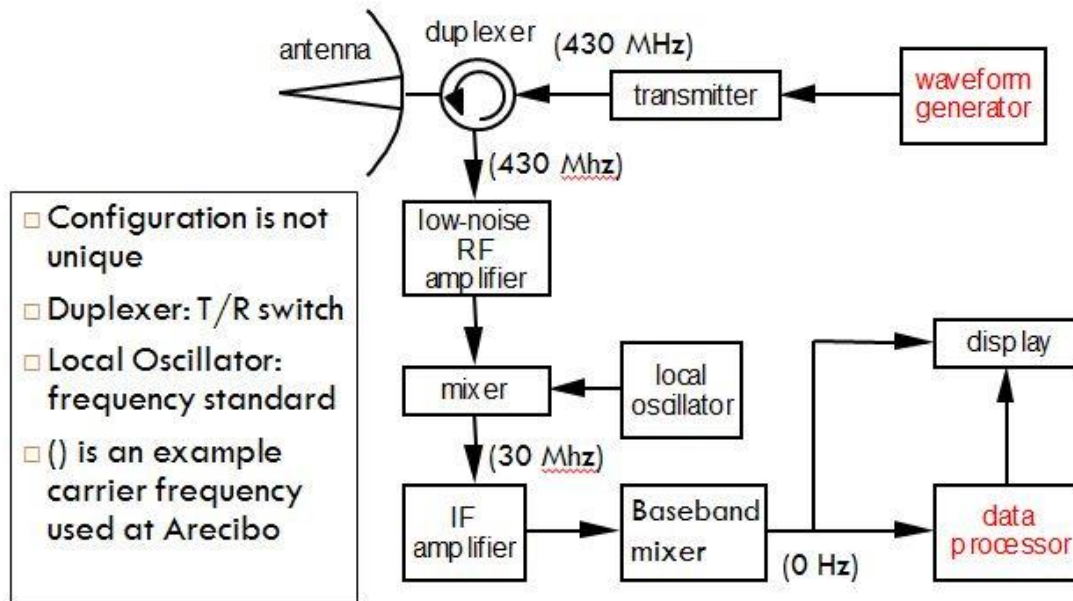


Figure 1: Simple pulsed monostatic radar at the AO operation frequency of 430 MHz. Adapted from Richards<sup>[14]</sup>.

The raw data extracted from received signal at AO was interpreted using MATLAB scripts written by Dr. Qihou H. Zhou that were modified to extract the desired data for analysis. The method analysis of the raw data is briefly described as follows:

The in-phase (I) and quadrature (Q) signals from one record (8 pulses) were converted to complex data for mathematical interpretation. For each pulse the S/R was computed using Equation (1) for each height, and then checked to see if it was greater than the predetermined threshold of 2.

$$SNR = \max\left(\frac{|complex\ data\ of\ one\ pulse|^2}{average\ power}\right) \quad (1)$$

Then if the length of the pulse was greater than or equal to 80% the length of the transmitted pulse (270 μs), multiplied by the gate width, it was determined to be a potential meteor and data was extracted.

This was done by cross-correlating the complex data of possible meteor with the complex conjugate of the transmitted pulse. The maximum of the absolute value of this cross-correlation

was then used to align the transmitted pulse and potential meteor data, and the product of these two is found.

Once data that appeared to be a meteor was found, various aspects of the received signal were calculated and extracted for further analysis. This was done to distinguish micro-meteors from noise, interference, and any other phenomena that may have triggered a false-positive. The two most vital aspects of the data were the height and velocity of the received signal. The height was determined using Equation (2), where  $g_d$  is the gate delay (476  $\mu$ s for this experiment),  $g_w$  is the gate width (1  $\mu$ s), and  $nT_x$  is the number of transmitted pulses.

$$Height = 0.15g_d + 0.15g_w(1 - nT_x) \quad (2)$$

The velocity was determined using Equation (3) where  $\Delta\phi$  is the mean phase shift of the received pulses.

$$v = \lfloor \frac{0.699*\Delta\phi}{4\pi g_w} \rfloor / 1000 \quad (3)$$

For consecutive meteor observations, the heights and velocities were compared to determine if they were the same meteor. Other aspects of the data that were extracted included the time of observation, SNR, mean phase shift, and standard deviation of the mean phase shift. Finally the data points with non-real (NaN) velocities were removed as these are the effects of incorrect data providing errors in the calculation. Additionally, reasonable filters were determined by analyzing the statistics of the resultant data set and from known restrictions. These filters will be discussed in greater detail in section 3.

## Results and Discussion

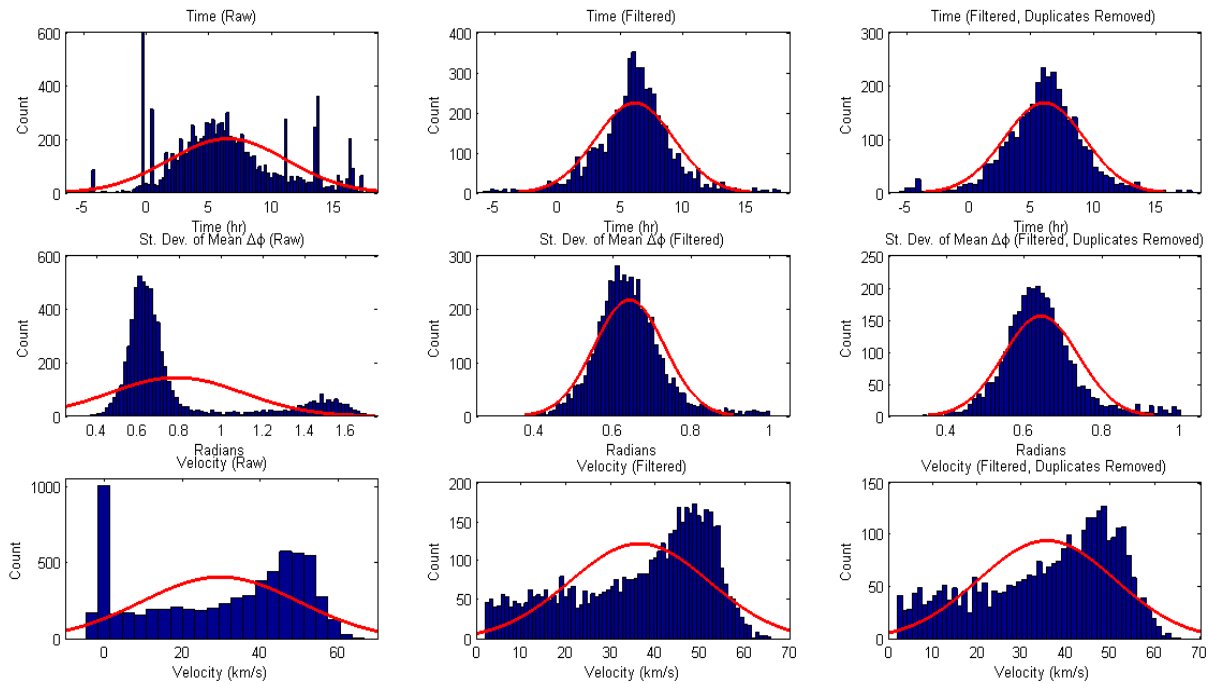


**Figure 2:** Histograms of the data before and after applying filters. Top (2a, 2b, 2c): Frequency of meteor observations for different times of day. Peak hours of observation occurred around 0600 suggesting the head echoes were the primary meteor echoes received. Hours -0500 to -0001 correspond to hours 1800 to 2359 respectively. Middle (2d, 2e, 2f): Frequency of the standard deviations of observed phase shift. The second bump around 1.5 radians was likely the result of interference (see Figure 5 below). Bottom (2g, 2h, 2i): Frequency of observed velocities. As expected, lower velocities created a near-uniform distribution, while most were observed with a velocity around 40 to 55 km/s<sup>[13]</sup>.

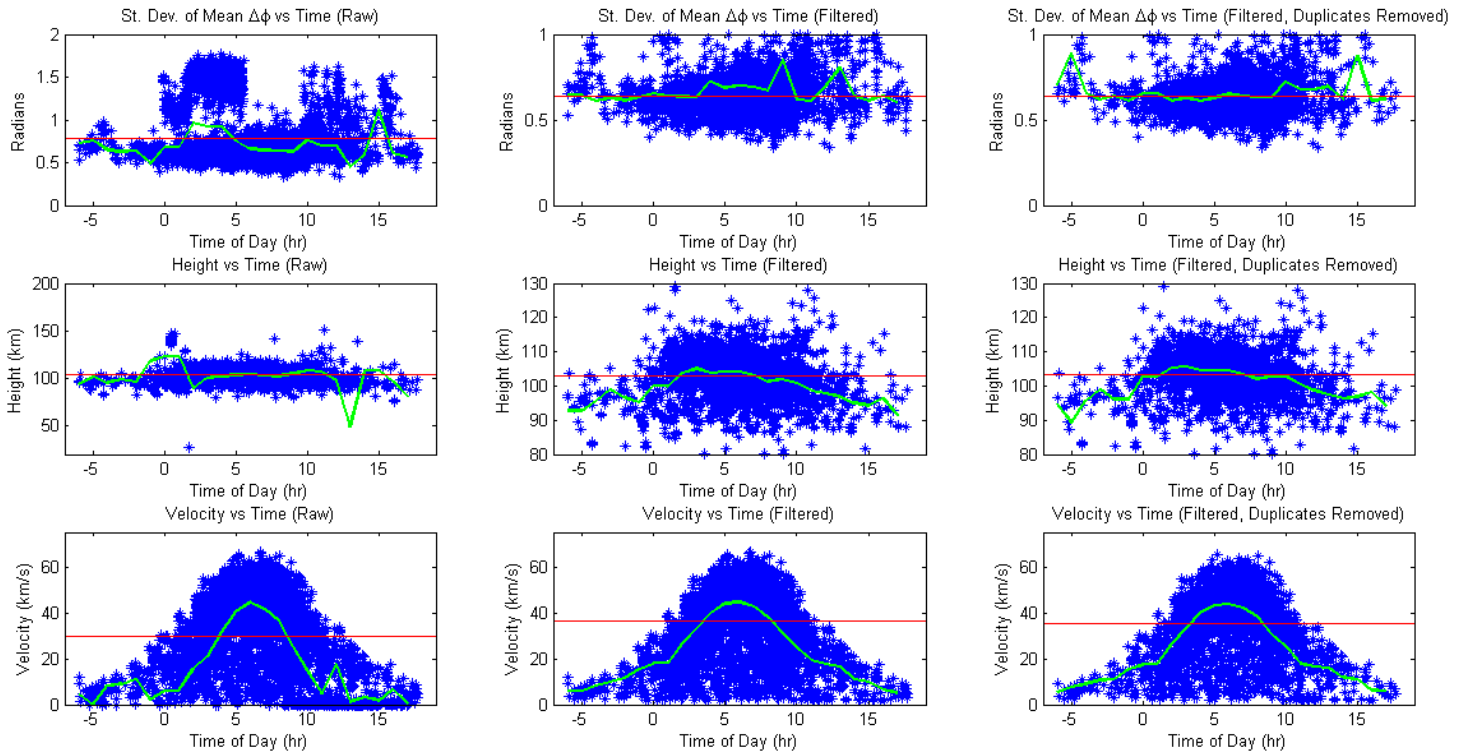


**Figure 3:** Plots of the variance of phase shift, height, and velocity vs. time before and after applying filters. The green line is the mean for the specific hour while the red line denotes mean of the entire data set. Top (3a, 3b, 3c): Variance of observed phase shift vs time of day. The fact that larger variances tended to cluster around the same time supports the hypothesis that there was interference in the received signal at those times. Middle (3d, 3e, 3f): Observed height vs time. It can be seen that even without the filter, few observations are made outside of the 80 to 120 km range expected.<sup>[9]</sup> Bottom (3g, 3h, 3i): Observed velocity vs time. Lower velocities (30 km/s and below) could be seen throughout the day, with peak velocities being observed near 0600 when the meteors would be moving into the apex<sup>[13]</sup>.

Raw, With duplicates					Raw, Without duplicates					Difference of Raw Data				
	Max	Min	Mean	St. Dev.		Max	Min	Mean	St. Dev.		Max	Min	Mean	St. Dev.
Time of Day (hr)	23.977	0.018889	8.5384	5.9901	Time	23.977	0	8.3478	5.643	Time	0	0.018889	0.1906	0.3471
Velocity (km/s)	162.21	-91.311	22.272	20.604	Vel	162.21	-91.311	21.507	19.83	Vel	0	0	0.765	0.774
SNR	8362.4	1.4348	77.781	402.99	SNR	7568.1	0	54.155	319.69	SNR	794.3	1.4348	23.626	83.3
Height (km)	167.85	27	98.801	26.322	Ht	167.85	0	100.07	25.418	Ht	0	27	-1.269	0.904
Mean $\Delta\phi$	2.9162	-1.6415	0.40041	0.37041	$\Delta\phi$	2.9162	-1.6415	0.38666	0.3565	$\Delta\phi$	0	0	0.01375	0.01391
St. Dev $\Delta\phi$	2.7466	0	0.72445	0.32396	Std $\Delta\phi$	2.7466	0	0.77189	0.36161	Std $\Delta\phi$	0	0	-0.04744	-0.03765
Filtered, With duplicates					Filtered, Without duplicates					Difference of Filtered Data				
	Max	Min	Mean	St. Dev.		Max	Min	Mean	St. Dev.		Max	Min	Mean	St. Dev.
Time of Day (hr)	23.977	0.018889	6.8862	3.8658	Time	23.977	0.030278	6.8325	3.921	Time	0	-0.01139	0.0537	-0.0552
Velocity (km/s)	66.513	2.022	36.349	15.511	Vel	65.416	2.069	35.438	15.285	Vel	1.097	-0.047	0.911	0.226
SNR	498.54	1.4348	35.089	71.871	SNR	498.54	1.4348	24.289	56.09	SNR	0	0	10.8	15.781
Height (km)	129	80.25	102.81	5.8036	Ht	129	80.25	103.44	5.8802	Ht	0	0	-0.63	-0.0766
Mean $\Delta\phi$	1.1958	0.036367	0.65349	0.27886	$\Delta\phi$	1.176	0.037214	0.6371	0.27479	$\Delta\phi$	0.0198	-0.00085	0.01639	0.00407
St. Dev $\Delta\phi$	0.99716	0.33708	0.63999	0.088999	Std $\Delta\phi$	0.99716	0.33708	0.63997	0.096249	Std $\Delta\phi$	0	0	2E-05	-0.00725
Max/Min Count	80.25				Max/Min	47.7273				Max/Min	32.5227			

**Figure 4:** Table of statistics with comparisons for raw data, filtered data, and data with duplicate observations filtered out.

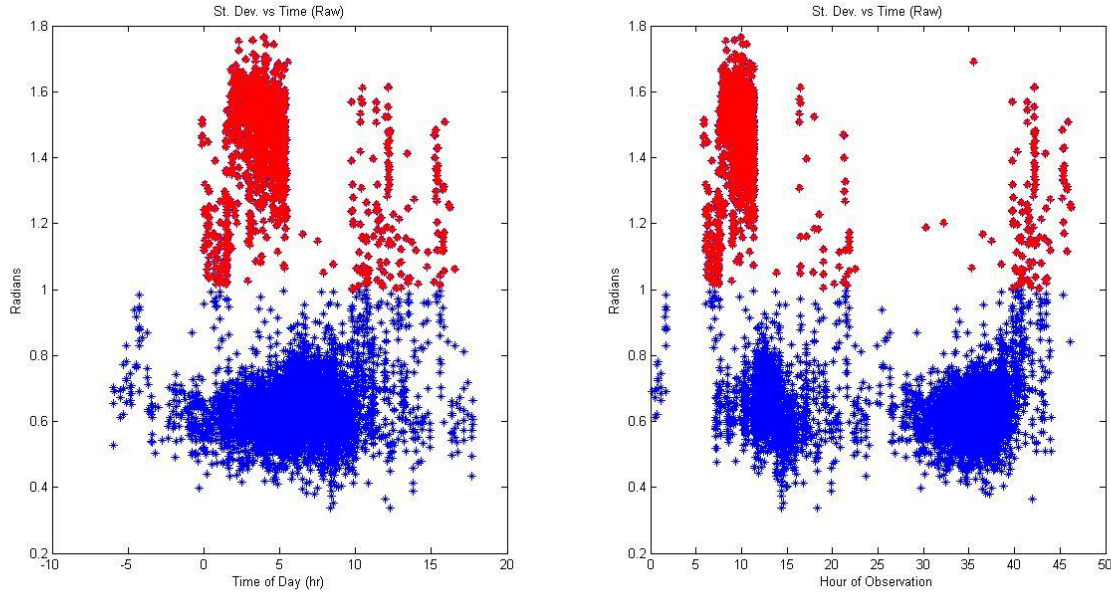


**Figure 5:** A closer look at the larger variance in average phase shift observed. In 5a (left) all 49 hours of observation are plotted by the time of day observed. 5b (right) looks at the breakdown of phase shift observed by the  $n$ th hour of observation, thus 0 corresponds to the beginning of the experiment. The 5th to 12th hour of observation where the spike in high variance of phase shift is observed corresponds to the hours of 2300 and 0600 suggesting that there was significant interference in the received signal.

The data was filtered by only looking at the observations between 80 km and 130 km in altitude. The lower limit is due to the fact that when a high power radar dish sends a signal, a bit of the signal “leaks” out of the edges of the dish and hits some of the ships out on sea by Puerto Rico and returns as a reflected signal. The reason why 80 km is selected as a filter threshold is through the fact that very few meteors are found below this altitude, as most burn up by the time they reach an altitude of about 95 km<sup>[2]</sup>. Therefore, the 80 km threshold helps define the difference between a ship detection and a meteor detection. The upper limit is because we observe the ionized trail created by the meteors ablating as they fall through the atmosphere. This ablation typically does not begin to occur until around 120 km due to infrequent collisions<sup>[9]</sup>, with only a small number ablating above 120 km as can be seen in Figures 3e and 3f.

The second filter applied was based on the standard deviation of the average phase shift observed. This is because the primary forces acting on the micro-meteors in Earth’s atmosphere are gravity and air resistance. Since the observed phase shift is used to determine the velocity of the meteor, and the meteor will be gradually slowing due to the air resistance, we know that we should not see any major deviations from the mean phase shift. From the raw data, the average variance of phase shift was 0.7245 with a standard deviation of 0.32. We chose to use one standard deviation above the mean variance of phase shift to filter out data that was likely erroneous. This decision is further supported by Figure 5, which shows the majority of these larger variances in observations occurred in a 6 hour observation window that was not seen

during the second day of observation. This strongly suggests that there was a source of interference that corrupted the collected data.

A similar filter was applied based on the mean SNR observed (77.78) plus one standard deviation (402.987), thus allowing for a maximum SNR of about 500. The reason for including this filter was because some of the SNRs received were  $10^3$  orders of magnitude larger than the median SNR of 6.5. This combined with the comparatively small mean and the standard deviation still an order of magnitude below the largest outliers led to the conclusion that these were unlikely to be meteor observations.

The final filter implemented was for velocity. We choose 90 km/s as the initial upper limit, although this proved largely unnecessary as even in the raw data, what few observations exceeded 60 km/s were well beyond 90 km/s. Thus, a strict upper limit of the filter seems to be unnecessary as it is unusual to see micro-meteors with velocities in excess of 60 km/s<sup>[9]</sup>. Still, we left the upper limit at 90 km/s to allow measurement errors as the maximum heliocentric velocity of meteors is typically confined to less than 71 km/s.

As can be seen from the bottom row of Figure 3, the raw velocity data was actually already in good agreement with the filtered as well as those found by other studies<sup>[10][11][12]</sup>, with the exception of the spike at very low velocities. This spike can be seen to correspond to the unusual spikes in observations around midnight, noon, 1400 and 1600. We know that the spike of observations near midnight occurred around hour 2337 for a period of 60 to 80 seconds and believe it to have been a military jet equipped with anti-radar technologies. For this spike as well as the others, none of the observed velocities exceeded 2 km/s, and many fluctuated around negative velocities near zero. Because it is rare to observe many low speed meteors, we imposed a 2 km/s lower limit on the velocity filter, as it was more likely to filter data that was not from a meteor echo than it was to filter actual meteors.

These filters overall produced results that were in good agreement with those found in other experiments<sup>[9][10][11][12]</sup>. Accounting for meteors observed multiple times before passing through the radar's beamwidth or burning up did not largely affect the meteor statistics observed. Figure 3 shows that the average heights and velocities of observed meteors changed little by removing duplicate observations and from Figure 4 it can be seen that deviation from this mean was also changed little by observing the meteors multiple times. However, the removal of duplicate observations did produce smoother histograms of the observations (Figure 2) as well as nearly halve the max-to-min observation ratio (Figure 4). Assuming the observation time is only a few days in length, it is probably safe to ignore the issue of duplicate observations with minimal error in the gathered statistics if quicker analysis is desirable.

The altitude of observations was primarily clustered between 95 and 110 km with a mean altitude of 103.44 km and is also in good agreement with previous experiments<sup>[1][9][10][12]</sup>. This is also where we expected to see the most due to ablation being less common near 120 km, and many meteors burning up near 95 km as discussed earlier.

Finally, we saw the greatest number of observations during the apex hours around 0600, forming a Gaussian distribution as anti-apex hours were approached. This is because of AO



concentrated beamwidth and high frequency being better able to detect head echoes rather than tail echoes<sup>[2]</sup>, and so apparent radiants near Earth's apex are the most likely to be detected<sup>[13]</sup>. This clustering of observations near 0600 has also been observed in a number of other studies<sup>[1][9][13]</sup>.

## Conclusion

Because of the agreement of our filtered data with observations from previous studies, we conclude that utilizing filters to extract data from 80 to 130 km in altitude, traveling at a velocity between 2 and 90 km/s effectively isolates micro-meteor observations. These observations can be further improved upon by filtering out those with phase shift variances near and above 1 radian, and abnormally high SNR. These observations helped verify micro-meteor trends and could potentially allow for multiple phenomena to be observed and provide a possible mathematical model for micro-meteors.

## Acknowledgements

We greatly acknowledge and thank the Arecibo Observatory staff for allowing us to conduct experiments at their facility as well as providing knowledge of known phenomenon in the area. We also extend thanks to Dr. Qihou Zhou for providing code to collect information from the raw data as well as his ongoing support and aide to our team.

## References

- [1] Zhou, Q., Tepley, C. A., & Sulzer, M. P. (1995). Meteor observations by the Arecibo 430 MHz incoherent scatter radar—I. Results from time-integrated observations. *Journal of Atmospheric and Terrestrial Physics*, 57(4), 421-431.
- [2] Mathews, J. D., Meisel, D. D., Hunter, K. P., Getman, V. S., & Zhou, Q. (1997). Very High Resolution Studies of Micrometeors Using the Arecibo 430 MHz Radar. *Icarus*, 126(1).
- [3] Lovell, A., & Clegg, J. A. (1948). Characteristics of Radio Echoes from Meteor Trails: I. The Intensity of the Radio Reflections and Electron Density in the Trails. *Proceedings of the Physical Society*, 60(5).
- [4] Opik, E.J. (1963). "Tables of Meteor Luminosities." *Irish Astronomical Journal*: vol 6 no. 1, 3-11.
- [5] Elford, W.G., and D.S. Robertson. (1953) "Measurements of Winds in the Upper Atmosphere by Means of Drifting Meteor Trails II." *Journal of Atmospheric and Terrestrial Physics*: 271-84.
- [6] Goodman, John M.(2005). "Operational Communication Systems and Relationships to the Ionosphere and Space Weather." *Advances in Space Research*: 2241-252.

- [7]Reinisch, B. W., D. M. Haines, K. Bibl, I. Galkin, X. Huang, D. F. Kitrosser, G. S. Sales, and J. L. Scali(1997). "Ionospheric Sounding in Support of Over-the-horizon Radar." *Radio Science*: 1681-694.
- [8]Zhou, Qihou H., and Michael C. Kelley(1997). "Meteor Observations by the Arecibo 430 MHz Incoherent Scatter Radar. II. Results from Time-resolved Observations." *Journal of Atmospheric and Solar-Terrestrial Physics*: 739-52.
- [9]Janches, D (2000). "Micrometeor Observations Using the Arecibo 430 MHz Radar I. Determination of the Ballistic Parameter from Measured Doppler Velocity and Deceleration Results." *Icarus*: 53-63.
- [10] Janches, Diego, Michael C. Nolan, David D. Meisel, John D. Mathews, Qihou H. Zhou, and Danielle E. Moser (2003). "On the Geocentric Micrometeor Velocity Distribution." *Journal of Geophysical Research*.
- [11] Janches, Diego, Sigrid Close, and Jonathan T. Fentzke (2008). "A Comparison of Detection Sensitivity between ALTAIR and Arecibo Meteor Observations: Can High Power and Large Aperture Radars Detect Low Velocity Meteor Head-echoes." *Icarus*: 105-11.
- [12] Janches, D., D. D. Meisel, and J. D. Mathews (2001). "Orbital Properties of the Arecibo Micrometeoroids at Earth Interception." *Icarus*: 206-18.
- [13] McIntosh, B.A., and A. Hajduk (1977) "Sunrise Effect on Persistent Radar Echoes from Sporadic Meteors." *Bulletin of the Astronomical Institute of Czechoslovakia* 28, no. 5 : 280-85. Accessed April 30, 2015.
- [14] Richards, M. (2005). Introduction to Radar Systems. In *Fundamentals of radar signal processing* (pp. 1-10). New York: McGraw-Hill